



Kevin C. Galbreath  
Principal Investigator

## TRANSITION METAL SPECIATION OF FOSSIL FUEL COMBUSTION FLUE GASES

**Key Project Personnel:** Kevin C. Galbreath (EERC), Jill M. Zola (EERC), Rokanuzzaman A.S.M. (EERC), Frank E. Huggins (University of Kentucky), and Gerald P. Huffman (University of Kentucky)

### *Project Description*

Chromium is a naturally occurring metallic element that exists primarily in two oxidation states: trivalent chromium ( $\text{Cr}^{3+}$ ) and hexavalent chromium ( $\text{Cr}^{6+}$ ).  $\text{Cr}^{3+}$  is an essential nutrient in human and animal diets and has very low toxicity.  $\text{Cr}^{6+}$  originates mostly from anthropogenic sources and is classified as a Group A inhalation carcinogen by the U.S. Environmental Protection Agency (EPA). Inhalation is the major human exposure pathway for  $\text{Cr}^{6+}$  [1]. X-ray absorption fine structure (XAFS) spectroscopy analyses indicate that  $\text{Cr}^{3+}$  is the dominant ( $\text{Cr}^{3+} > 95\%$  of the total Cr) species in bituminous coal and residual (No. 6 fuel) oil fly ashes (ROFAs) [2–5]. However, Cr XAFS measurements of western U.S. subbituminous coal fly ashes are lacking. Limited Cr XAFS measurements of a Powder River Basin (PRB) Wyodak coal and ash (ashed at  $500^\circ\text{C}$  in air for 24 hr) and Absaloka coal and fly ashes produced in a 7-kW combustion system indicate that maceral-bound  $\text{Cr}^{3+}$  occurs in the coals and on average  $52 \pm 5\%$  and  $43\%$ , respectively, of the total ash Cr occurs as  $\text{Cr}^{6+}$  [2, 6]. Additional Cr XAFS analyses of four western U.S. subbituminous coal fly ashes produced in a 50-kW combustion system indicated that  $\text{Cr}^{6+}$  accounted for approximately 10% to 30% of the total Cr contents [5]. These  $\text{Cr}^{6+}$  proportions are much larger than previous XAFS measurements of bituminous coal fly ashes ( $\text{Cr}^{6+} < 5\%$  of the total Cr) produced under typical coal combustion conditions [2, 3, 5, 6]. As part of this investigation, five PRB coal fly ashes collected from utility-scale power plants equipped with different furnace configurations, but similar cold-side electrostatic precipitators (ESPs) were analyzed using XAFS to confirm whether western U.S. subbituminous coal fly ashes contain greater proportions of  $\text{Cr}^{6+}$  relative to eastern U.S. bituminous coal fly ashes. Thermodynamic modeling was also used to investigate whether differences in bituminous and subbituminous coal compositions control the formation of  $\text{Cr}^{6+}$ . Differences in coal Cr modes of occurrence were also considered to explain variations in  $\text{Cr}^{6+}$  concentrations.

The fly ash produced from residual (No. 6 fuel) oil combustion contributes to airborne particulate matter (PM). Controlling residual oil fly ash (ROFA) emissions, however, is difficult because a substantial fraction of ROFA particles is generally submicron, corresponding to the size range of 0.1 to  $1 \mu\text{m}$ , where existing industrial gas-cleaning devices are least effective. XAFS and x-ray diffraction (XRD) analyses of ROFA indicate that  $\text{NiSO}_4 \cdot x\text{H}_2\text{O}$  and Ni-bearing oxide spinel (possibly,  $\text{NiFe}_2\text{O}_4$ ) are the dominant Ni species [4, 7–9]. Evidence presented by Galbreath et al. [8] suggests that the addition of magnesium hydroxide ( $\text{Mg}[\text{OH}]_2$ ) to residual oil, added to suppress sulfuric acid mist formation and coke formation and promote the formation of friable deposits, impedes nickel sulfation and promotes  $\text{NiFe}_2\text{O}_4$  formation during the combustion and/or ash formation process. The presence of a nickel oxide compound, such as  $\text{NiFe}_2\text{O}_4$ ,

may increase future inhalation health risk estimates because its carcinogenicity is unknown, whereas  $\text{NiSO}_4 \cdot x\text{H}_2\text{O}$  is noncarcinogenic [10, 11]. Thermodynamic modeling was used to evaluate the potential effects of  $\text{Mg}(\text{OH})_2$  injection on the Ni speciation of ROFA.

### ***Goal***

Project goals are threefold:

1. Determine whether PRB subbituminous coal fly ashes contain greater proportions of  $\text{Cr}^{6+}$  relative to bituminous coal fly ashes.
2. Evaluate the roles of coal chemical compositions and Cr modes of occurrence on Cr oxidation.
3. Evaluate the effects of  $\text{Mg}(\text{OH})_2$  injection on the Ni speciation of ROFA.

### ***Rationale***

In the United States, the impetus for focusing on individual elements, such as Cr and Ni, in air pollution derives from the 1990 Clean Air Act Amendments (CAAA) [12] and the attainment of National Ambient Air Quality Standards [13]. Title III of the CAAA identifies 189 chemicals (later revised to 188), including Cr and Ni and 14 other inorganic trace elements (As, Be, Cd, Cl, Co, F, Hg, Mn, P, Pb, Sb, Se, Th, and U), as potential hazardous air pollutants (HAPs) or air toxics. EPA's Integrated Urban Air Toxics Strategy also classifies Cr and Ni as urban HAPs [14]. Many stationary sources have had to report Cr and Ni emissions as part of the EPA Toxics Release Inventory (TRI) [15]. Although TRI and similar reporting provide estimates of the amounts of Cr and Ni released into the environment, they are not an indicator of toxicity because the acute, chronic, and cancer-causing effects vary significantly for the different chemical species of Cr and Ni.

Although chemical equilibrium is probably not attained in such a dynamic system as a utility-scale combustion flue gas, an equilibrium analysis provides useful information on speciation and mass distributions toward which chemical reactions proceed under given conditions of temperature, pressure, and composition. Given that actual coal combustion conditions are subject to kinetic control, the results of this equilibrium investigation are useful for future development of Cr and Ni reaction schemes for kinetic models.

### ***Approach***

Five representative PRB fly ash samples from power plants with different furnace configurations, described in Table 1, but similar cold-side ESP were obtained from the Energy & Environmental Research Center Coal Ash Resources Research Consortium. Cr contents of the fly ash samples were determined using microwave-assisted acid digestion (EPA Method 3050 and American Society for Testing and Materials Standard Practice D 5513) followed by inductively coupled plasma–mass spectrometry.

Coal fly ash  $\text{Cr}^{3+}/\text{Cr}^{6+}$  were determined using Cr K-edge XAFS at beam-line 4-3 of the Stanford Synchrotron Radiation Laboratory, Stanford University, California. A representative portion of each coal fly ash sample (~200 mg) was suspended in the x-ray beam in an envelope made of ultrathin polypropylene. Absorption data were collected from such sample in fluorescence geometry using a 13-element Ge detector, which was gated electronically to receive predominantly the x-rays fluoresced by Cr. A 6- $\mu\text{m}$  V filter and

**Table 1.** PRB Subbituminous Coal Fly Ash Source Information

Fly Ash No.	Fuel	Furnace Type
1	92% North Antelope–8% petroleum coke	Wet bottom cyclone
2	95% North Antelope–5% Antelope	Dry bottom, front-fired, pulverized coal
3	Black Thunder	Dry bottom, tangential-fired, pulverized coal
4 and 5	Spring Creek	Dry bottom, tangential- and front-fired, pulverized coal

soller slits were also employed to enhance the signal/noise ratio. Cr XAFS spectra were collected as a function of energy at a stepping interval of 0.25 eV over a range from 5889 to 6389 eV, that is, from -10 to +40 eV with respect to the Cr K absorption edge at 5989 eV. The spectral region from -10 to +40 eV is referred as the x-ray absorption near edge structure (XANES) region. For each sample, Cr K-edge XAFS spectra were accumulated at least 4 times to improve the signal-to-noise ratio. The first major derivative in the XAFS spectrum of a thin chromium foil defined the Cr K-edge at 5989 eV, and the energy scales for the fly ash spectra were calibrated accordingly.

A thermodynamic model, the Facility for Analysis of Chemical Thermodynamics (FACT), was used to investigate potential differences in the  $\text{Cr}^{3+}/\text{Cr}^{6+}$  of bituminous and PRB subbituminous coal fly ashes. Comprehensive equilibrium gas-phase calculations similar to those of Kashireninov and Fontijn [16] were performed, with emphasis on  $\text{Cr}^{6+}$  behavior. Representative bituminous and PRB subbituminous flue gas and fly ash compositions were used to investigate whether compositional differences and chemical equilibrium conditions can explain potential variations in  $\text{Cr}^{3+}/\text{Cr}^{6+}$ . Differences in coal Cr modes of occurrence were also considered in explaining potential differences in the Cr speciation of bituminous and subbituminous coal fly ashes. FACT was also used to model the apparent effect of a  $\text{Mg}(\text{OH})_2$  oil additive on Ni sulfation reactions. The  $\text{Mg}(\text{OH})_2$  injection rate into an oil-fired unit may be optimized to promote Ni sulfation and suppress the formation of  $\text{NiFe}_2\text{O}_4$ , a suspected carcinogen.

## Progress

### XAFS Cr Speciation Measurements

As indicated in Table 2, the five PRB coal fly ash samples contain between about 47 and 79 ppm Cr. As a quality control (QC) measure, a National Institute of Standards and Technology (NIST) Standard Reference Material (SRM) 1633b, bituminous coal fly ash, was analyzed in duplicate for its Cr content. The average measured value of 194 ppm compared favorably with a relative difference of -2.1% from the NIST SRM certified value of  $198.2 \pm 4.7$  ppm.

Presented in Figure 1 are the Cr K-edge XANES spectra for the five PRB coal fly ashes. As discussed in more detail elsewhere [2], the peak at about 2 eV in Figure 1 represents a small, weakly localized transition involving  $\text{Cr}^{3+}$ , whereas the peak at 4 eV represents a composite peak for an even smaller  $\text{Cr}^{3+}$  transition peak and a much more intense peak associated with the presence of  $\text{Cr}^{6+}$ . By measuring the relative heights of these two peaks for mixtures containing known amounts of  $\text{Cr}^{3+}$  and  $\text{Cr}^{6+}$ , a calibration curve was developed that relates peak heights to the fraction of Cr present as  $\text{Cr}^{6+}$  in the sample [2]. Peak intensities were measured using an iterative least-squares fitting technique involving a mathematical function based on two peaks of mixed Lorentzian-Gaussian line shape and an arctangent curve for the background produced by the Cr absorption edge. An example of results from the iterative least-squares fitting technique is shown in Figure 2. Presented in Table 3 are the measured peak intensities and the relative proportions and

**Table 2.** Average of Duplicate Cr Analysis Results

PRB Coal Fly Ash	Cr, ppm
1	67.3
2	76.1
3	78.9
4	60
5	47

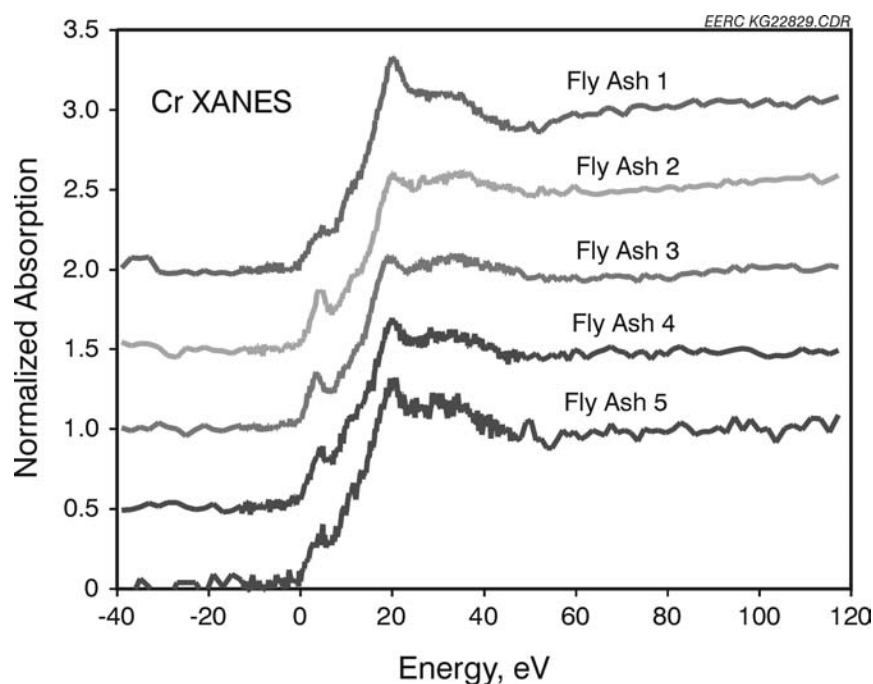


Figure 1. Cr K-Edge XANES Spectra for the Five PRB Subbituminous Coal Fly Ashes

concentrations of  $\text{Cr}^{6+}$  in the five PRB coal fly ashes. The estimated uncertainty in the  $\text{Cr}^{6+}$  determinations is  $\pm 5\%$ . The range of  $\text{Cr}^{6+}$  proportions in Table 3, approximately 10% to 30%, is consistent with the values of 10% to 30%  $\text{Cr}^{6+}$  reported by Shoji et al. [5] for four western U.S. subbituminous coal fly ashes produced in a 50-kW combustion system. The  $\text{Cr}^{6+}$  proportions in Table 3, however, are significantly less than the  $52 \pm 5\%$  and 43%  $\text{Cr}^{6+}$  values reported for the PRB Wyodak and Absaloka coal fly ashes, respectively [2, 6]. The proportions of  $\text{Cr}^{6+}$  measured in this investigation support the hypothesis that western U.S. PRB subbituminous coal fly ashes contain greater proportions of  $\text{Cr}^{6+}$  relative to eastern U.S. bituminous coal fly ashes.

#### **Thermodynamic Modeling of Cr Speciation in Western U.S. Subbituminous and Eastern U.S. Bituminous Coals**

The chemical compositions of PRB subbituminous Absaloka and bituminous Illinois No. 6 coals, presented in Tables 4–6, were used as FACT input. XAFS analyses of fly ashes produced from the combustion of these two coals in a 7-kW system indicated that 43% of the 130 ppm Cr in Absaloka fly ash

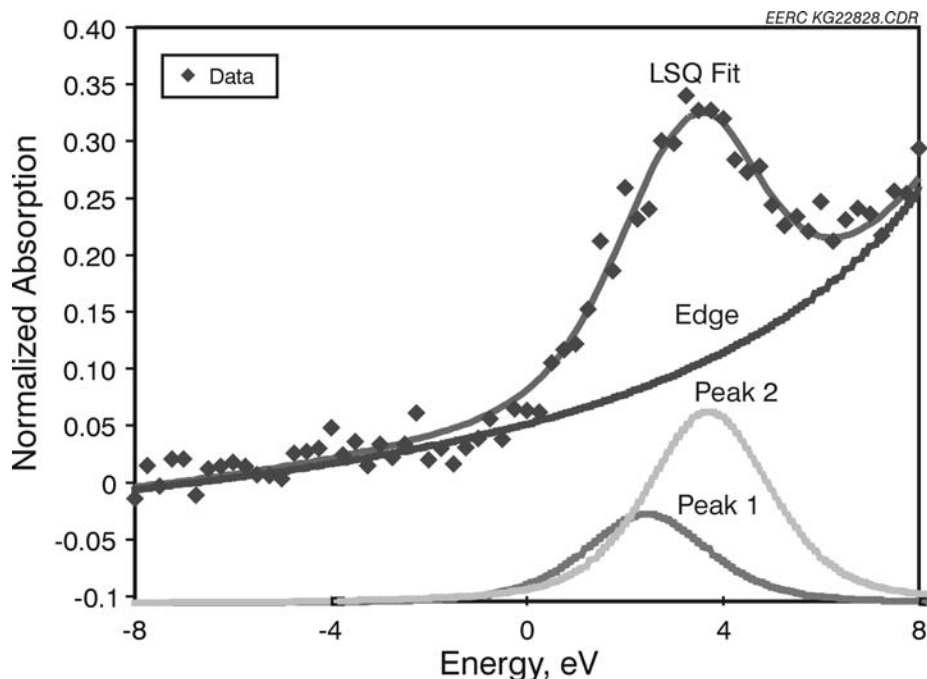


Figure 2. Iterative Least-Squares Fit Results for a Cr K-Edge XANES Spectrum of a PRB Subbituminous Coal Fly Ash

**Table 3.** Least-Squares Cr XANES Analysis Results

PRB Coal Fly Ash	2–3 eV Peak Intensity, $I_2$	4–5 eV Peak Intensity, $I_4$	$\text{Cr}^{6+}$ , % of total $\text{Cr}^{\text{I}}$	$\text{Cr}^{6+}$ , ppm
1	0.115	0.148	$12 \pm 5$	$8 \pm 3$
2	0.027	0.254	$27 \pm 5$	$20 \pm 4$
3	0.079	0.169	$16 \pm 5$	$13 \pm 4$
4	0.074	0.145	$13 \pm 5$	$8 \pm 3$
5	0.12	0.133	$10 \pm 5$	$5 \pm 2$

<sup>1</sup> Calculated from  $\text{Cr}^{6+} = 110(I_4 - I_2/3)$ , where  $I_4$  and  $I_2$  are XANES peak intensities at 4–5 and 2–3 eV, respectively.

was present as  $\text{Cr}^{6+}$  compared to only 6% of the 170 ppm Cr in Illinois No. 6 fly ash [6]. Combustion conditions used during the production of Absaloka and Illinois No. 6 coal fly ashes, that is pressure of 1 atm, temperature range of 100° to 1500°C, and an excess air concentration of 20 mol%, were considered in the equilibrium calculations. Equilibria among the solid (s) and gaseous (g) Cr species identified in Table 7 were calculated assuming ideal gas mixtures and pure condensed species. A given species was considered only within the temperature range for which thermochemical data exist; i.e., data extrapolation was not performed. Predicted Cr species equilibria for the Absaloka and Illinois No. 6 coal combustion flue gases are presented in Figures 3 and 4, respectively. Above 1100°C,  $\text{Cr}^{4+}$  and  $\text{Cr}^{6+}$  oxide species,  $\text{CrO}_2$  and  $\text{CrO}_3$ , respectively, are the dominant gas species in both flue gases.  $\text{CrO}_3(\text{g})$  is predicted to be stable only at very high temperatures and not at stack temperatures. Oxide spinel phases containing  $\text{Cr}^{3+}$ ,  $\text{FeCr}_2\text{O}_4$  and/or  $\text{MgCr}_2\text{O}_4$ , are the first solid phases to form in both flue gases. The  $\text{Cr}^{3+}$ -bearing  $\text{Cr}_2\text{O}_3(\text{s})$  phase is predicted to form in

**Table 4.** Coal Proximate Analysis Results, as-received wt%

Analysis Parameters	Illinois No. 6	Absaloka
Volatile Matter	34.4	36.2
Fixed Carbon	43.7	33.4
Ash	14.6	9.34
Higher Heating Value, MJ/kg	26.03	20.28

**Table 5.** Coal Ultimate Analysis Results, as-received wt%

Analysis Parameters	Illinois No. 6	Absaloka
Carbon	61.5	49.4
Hydrogen <sup>1</sup>	4.29	2.63
Nitrogen	1.00	1.07
Sulfur	4.27	0.78
Ash	14.6	9.34
Oxygen (by difference) <sup>1</sup>	7.07	15.8
Total Moisture	7.30	21.0

<sup>1</sup> As-received hydrogen and oxygen do not include the H and O in sample moisture.

**Table 6.** Comparison of Coal Major and Minor Elemental Oxide Compositions, ash wt%

Elemental Oxide	Illinois No. 6	Absaloka
SiO <sub>2</sub>	40.1	25.7
Al <sub>2</sub> O <sub>3</sub>	19.5	17.2
Fe <sub>2</sub> O <sub>3</sub>	14.5	5.28
TiO <sub>2</sub>	1.0	0.85
P <sub>2</sub> O <sub>5</sub>	0.3	0.35
CaO	7.5	30.9
MgO	2.4	3.30
Na <sub>2</sub> O	1.4	1.47
K <sub>2</sub> O	1.6	0.47
SO <sub>3</sub>	11.7	17.6
Total	100.0	103.1

**Table 7.** Chromium Species Considered in Equilibrium Analysis

Species
Cr(s,g), CrO(g), CrO <sub>2</sub> (s,g), CrO <sub>3</sub> (s,g), Cr <sub>2</sub> O <sub>3</sub> (s), Cr <sub>3</sub> O <sub>4</sub> (s), Cr <sub>5</sub> O <sub>12</sub> (s), Cr <sub>8</sub> O <sub>21</sub> (s), Cr <sub>3</sub> C <sub>2</sub> (s), Cr <sub>4</sub> C(s), Cr <sub>7</sub> C <sub>3</sub> (s), Cr <sub>23</sub> C <sub>6</sub> (s), Cr(CO) <sub>6</sub> (s), CrN(s,g), Cr <sub>2</sub> N(s), CrS(s,g), Cr <sub>2</sub> S <sub>3</sub> (s), Cr <sub>3</sub> S <sub>4</sub> (s), Cr <sub>5</sub> S <sub>6</sub> (s), Cr <sub>6</sub> S <sub>7</sub> (s), Cr <sub>2</sub> (SO <sub>4</sub> ) <sub>3</sub> (s), CrCl <sub>2</sub> (s), CrCl <sub>3</sub> (s), CrO <sub>2</sub> Cl <sub>2</sub> (g), NiCr <sub>2</sub> O <sub>4</sub> (s), FeCr <sub>2</sub> O <sub>4</sub> , MgCr <sub>2</sub> O <sub>4</sub>

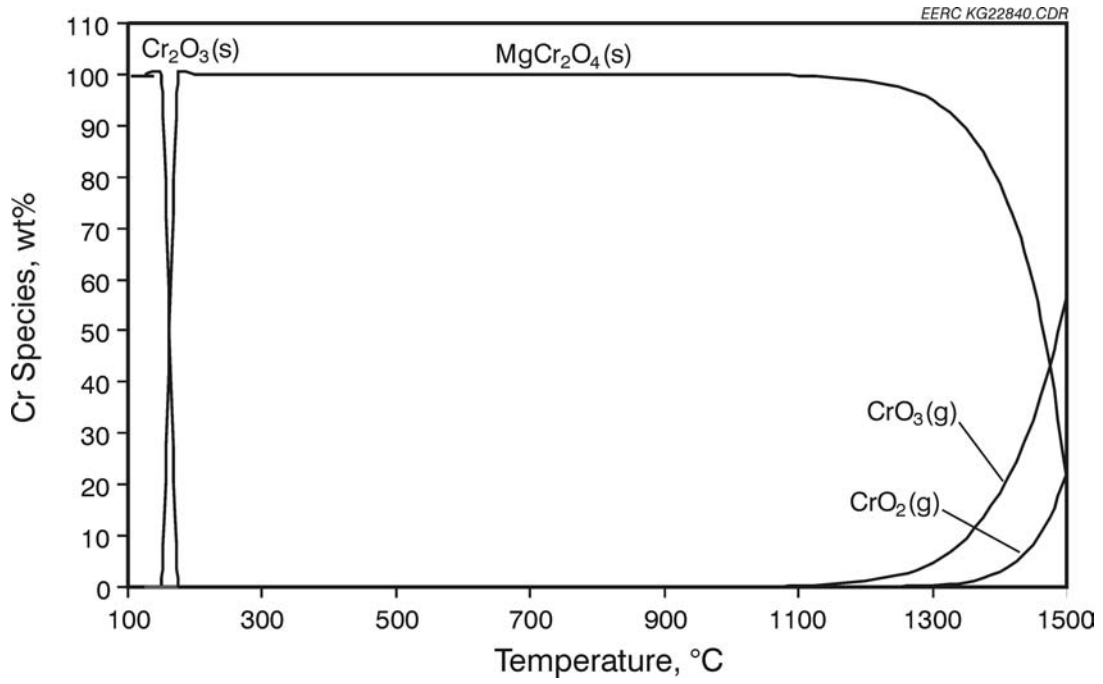


Figure 3. Predicted Cr Speciation Distribution of Absaloka Coal Combustion Flue Gas

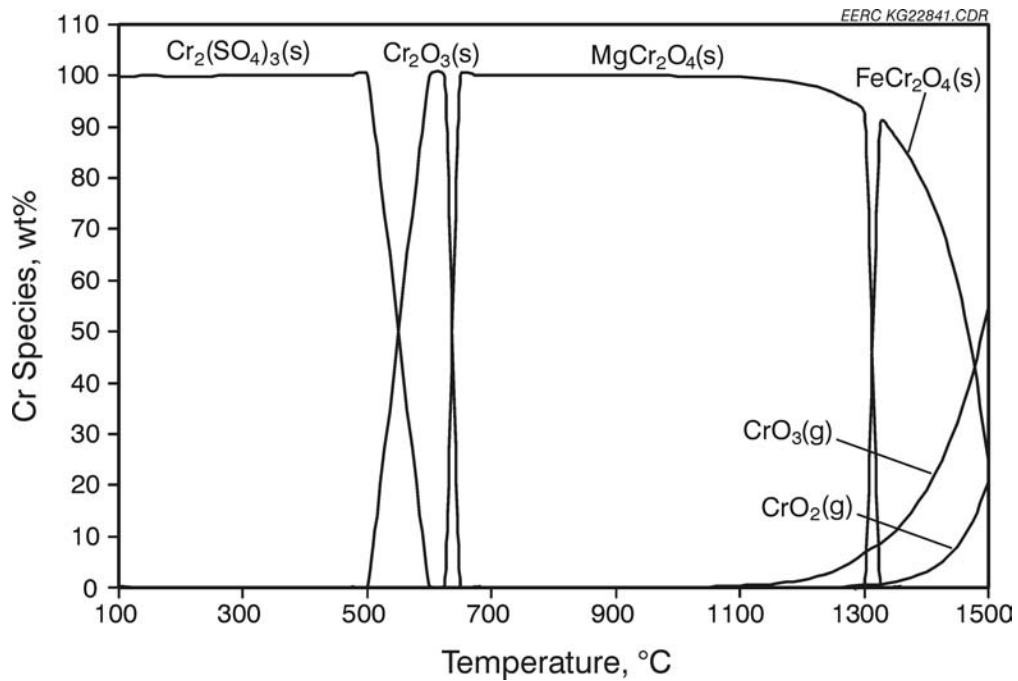


Figure 4. Predicted Cr Speciation Distribution of Illinois No. 6 Coal Combustion Flue Gas

both flue gases at lower temperatures, but in the Illinois No. 6 fly ash,  $\text{Cr}_2\text{O}_3(\text{s})$  becomes sulfated at  $\leq 500^\circ\text{C}$  because of the much higher sulfur content of this bituminous coal relative to the PRB coal (Table 5).  $\text{Cr}^{6+}$  phases are not predicted to occur in PRB subbituminous Absaloka or bituminous Illinois No. 6 coal fly ashes.

FACT modeling did not accurately predict differences in eastern U.S. bituminous and western U.S. subbituminous coal fly ash  $\text{Cr}^{6+}$  contents, suggesting that coal chemical compositional differences alone cannot account for  $\text{Cr}^{6+}$  formation. The oxidation state of Cr is probably dictated more by mineralogical and mode of occurrence differences between the eastern U.S. bituminous and western U.S. PRB subbituminous coals. The predominance of maceral-bound  $\text{Cr}^{3+}$ , oxygen functional groups, and carboxyl-bound alkaline earth metals, primarily Ca and Mg, in western U.S. subbituminous coals may promote  $\text{Cr}^{6+}$  formation, perhaps as a Ca- and/or Mg-based chromate compound (e.g.,  $[\text{Ca}, \text{Mg}]\text{CrO}_4$ ).

### Thermodynamic Modeling of Ni Speciation in Residual Oil Fly Ash

The residual oil chemical composition in Table 8 and compositions of ROFAs, before and after  $\text{Mg}(\text{OH})_2$  oil injection, in Table 9 were used as input into FACT. These compositions were obtained from a residual oil and ROFAs sampled from a 400-MW boiler unit [8]. XRD analyses of the ROFAs indicated that the injected  $\text{Mg}(\text{OH})_2$  reacts with  $\text{SO}_2$  and  $\text{SO}_3$  in the flue gas to form  $\text{MgSO}_4 \cdot 6\text{H}_2\text{O}$  [8]. Consequently, in addition to the 35 Ni species identified in Table 10, equilibria among  $\text{MgSO}_4 \cdot 6\text{H}_2\text{O}$  and about 40 other Mg-containing compounds were considered in the calculations. Similar to the Cr speciation calculations, a given species was considered only within the temperature range for which thermochemical equilibrium data exist. Combustion conditions at the power plant, that is pressure of 1 atm, temperature range of  $100^\circ$  to  $1500^\circ\text{C}$ , and an excess air concentration of 4 mol%, were considered in the calculations. Predicted Ni species equilibria for the ROFAs before and after the addition of  $\text{Mg}(\text{OH})_2$  are presented in Figures 5 and 6, respectively. A comparison of Figures 5 and 6 indicates that the addition of  $\text{Mg}(\text{OH})_2$  did not impede Ni sulfation, that is the formation of  $\text{NiSO}_4$ , apparently because of an excess in sulfur despite the formation of  $\text{MgSO}_4 \cdot 6\text{H}_2\text{O}$ .  $\text{Mg}(\text{OH})_2$  addition actually extended the onset of Ni sulfation from  $650^\circ$  to  $700^\circ\text{C}$ .  $\text{Mg}(\text{OH})_2$  addition also extended the onset of  $\text{NiAl}_2\text{O}_4$  formation from  $800^\circ$  to  $1250^\circ\text{C}$  at the expense of  $\text{Ni}_2\text{SiO}_4$ . In the presence of additional Mg,  $\text{Mg}_2\text{SiO}_4$  replaced  $\text{Ni}_2\text{SiO}_4$  as a dominant high-temperature phase.

**Table 8.** Residual Oil Ultimate Analysis Results

Analysis Parameters	As-Received, wt%
Carbon	86.7
Hydrogen	9.91
Nitrogen	0.83
Sulfur	1.44
Ash	0.14
Oxygen	1.01

**Table 9.** Residual Oil Major and Minor Elemental Oxide Compositions, ash wt%

Elemental Oxide	Baseline	After Mg(OH) <sub>2</sub> Addition
SiO <sub>2</sub>	40.8	29.8
Al <sub>2</sub> O <sub>3</sub>	12.3	9.00
Fe <sub>2</sub> O <sub>3</sub>	5.19	3.79
NiO	6.10	4.46
V <sub>2</sub> O <sub>5</sub>	14.6	10.6
CaO	14.2	10.4
MgO	1.65	28.1
Na <sub>2</sub> O	5.14	3.76
K <sub>2</sub> O	<0.10	<0.1
Total	99.98	99.91

**Table 10.** Nickel Species Considered in Equilibrium Analysis

Ni(s,g)	Ni <sub>2</sub> Al <sub>3</sub> (s)	Ni <sub>4</sub> SO <sub>4</sub> (OH) <sub>6</sub> (s)
NiH(g)	Ni <sub>3</sub> Al(s)	Ni <sub>7</sub> (SO <sub>4</sub> ) <sub>3</sub> (OH) <sub>8</sub> (s)
Ni <sub>2</sub> H(s)	Ni(OH) <sub>2</sub> (s,g)	Ni(N <sub>2</sub> H <sub>4</sub> ) <sub>3</sub> SO <sub>4</sub> (s)
Ni <sub>3</sub> C(s)	NiS(s,g)	Ni <sub>2</sub> Fe(CN) <sub>6</sub> (s)
NiO(s,g)	NiS <sub>2</sub> (s)	NiAl <sub>2</sub> O <sub>4</sub> (s)
NiOOH(s)	Ni <sub>3</sub> S <sub>2</sub> (s)	NiCl(g)
NiO <sub>2</sub> (H <sub>2</sub> O)(s)	Ni <sub>3</sub> S <sub>4</sub> (s)	NiCl <sub>2</sub> (s,g)
Ni(CO) <sub>4</sub> (g)	Ni <sub>6</sub> S <sub>5</sub> (s)	NiFe <sub>2</sub> O <sub>4</sub> (s)
NiCO <sub>3</sub> (s)	NiSO <sub>4</sub> (s)	NiCr <sub>2</sub> O <sub>4</sub> (s)
MgNi <sub>2</sub> (s)	NiSO <sub>4</sub> · H <sub>2</sub> O(s)	NiSi(s)
NiAl(s)	NiSO <sub>4</sub> · 6H <sub>2</sub> O(s)	Ni <sub>2</sub> Si(s)
NiAl <sub>3</sub> (s)	NiSO <sub>4</sub> · 7H <sub>2</sub> O(s)	Ni <sub>7</sub> Si <sub>13</sub> (s)
		Ni <sub>2</sub> SiO <sub>4</sub> (s)

**Status**

Project was completed during the summer of 2003.

**Quality Assurance/Quality Control**

As a QC measure, a NIST SRM 1633b, bituminous coal fly ash, was analyzed in duplicate for its Cr content. The average measured value of 194 ppm compared favorably with a relative difference of -2.1% from the NIST SRM certified value of 198.2 ± 4.7 ppm. The estimated uncertainty in the XAFS Cr<sup>6+</sup> determinations was ± 5% based on x-ray counting statistics.

**Potential Users/Technology Transfer**

Knowledge of the Cr and Ni species being released by coal- and oil-burning power systems will ultimately result in a more realistic inhalation-based health risk assessment for the utility industry. Such an assessment is necessary for EPA to properly address public concerns about potential health risks and

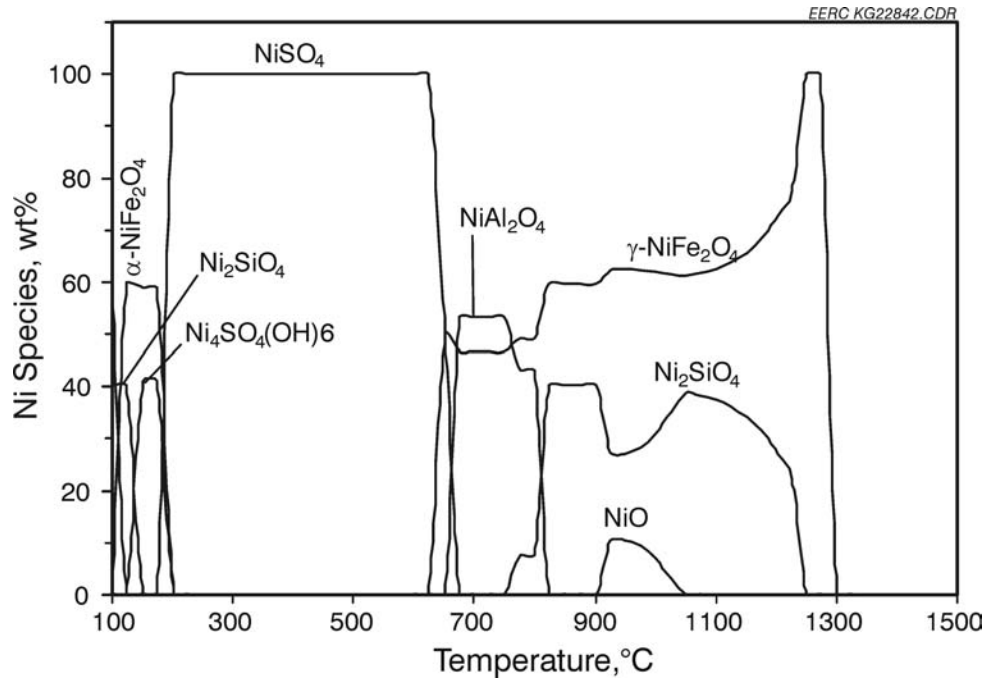


Figure 5. Predicted Ni Speciation Distribution of Baseline ROFA

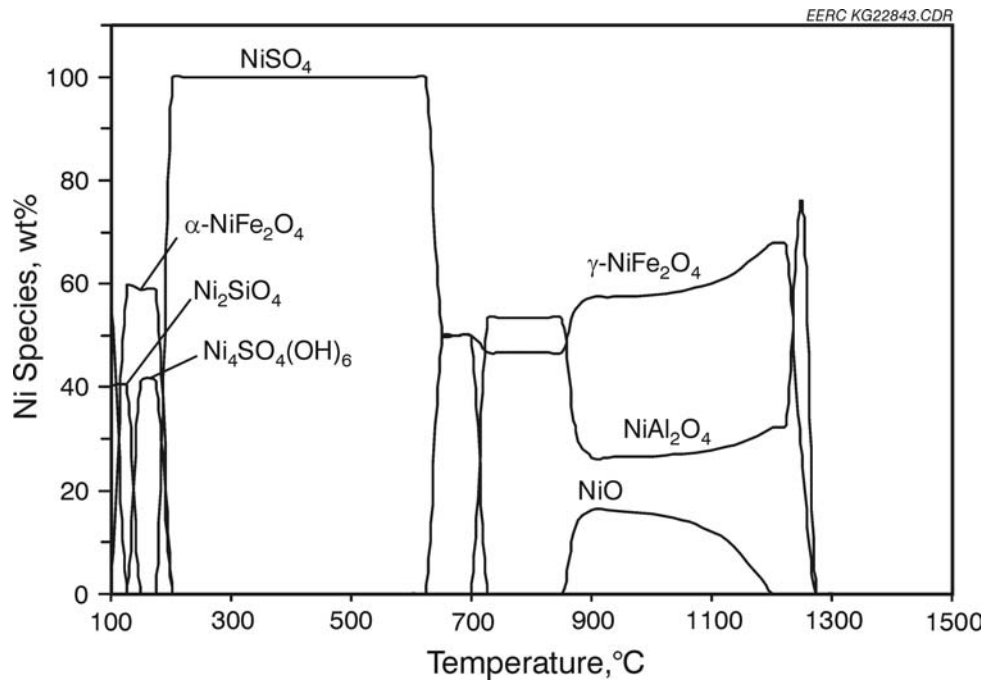


Figure 6. Predicted Ni Speciation Distribution of Mg-Rich ROFA

regulatory decisions for fossil fuel-burning boilers. In addition, a Cr and Ni speciation release inventory will enable industry stakeholders to focus on the relative toxicity and health risk of Ni and Cr releases, taking into consideration the specific chemical forms of these releases, rather than the total quantities reported in EPA's TRI. Additional chemical speciation results are also useful for improving Ni and Cr emission control strategies, should it become necessary, because each metal species has distinctive physical and chemical properties. Emerging issues such as the role of transition metals in health effect mechanisms associated with exposure to fine PM may increase the importance of controlling Cr, Ni, and other transition metal emissions.

### References

1. Agency for Toxic Substances and Disease Registry, Toxicological Profile for Chromium, September 2000. Atlanta, GA: U.S. Department of Health and Human Services, Public Health Service.
2. Huggins, F.E.; Najih, M.; Huffman, G.P. Direct Speciation of Chromium in Coal Combustion By-Products by X-Ray Absorption Fine-Structure Spectroscopy. *Fuel* **1999**, *78*, 233–242.
3. Huggins, F.E.; Shah, N.; Huffman, G.P.; Robertson, J.D. XAFS Spectroscopic Characterization of Elements in Combustion Ash and Fine Particulate Matter. *Fuel Processing Technology* **2000**, *65–66*, 203–218.
4. Galbreath, K.C.; Zygarlicke, C.J.; Toman, D.L.; Huggins, F.E.; Huffman, G.P. Nickel and Chromium Speciation of Residual Oil Combustion Ash. *Combustion Science and Technology* **1998**, *134 (1–6)*, 243–262.
5. Shoji, T.; Huggins, F.E.; Huffman, G.P.; Linak, W.P.; Miller, A.C. XAFS Spectroscopy Analysis of Selected Elements in Fine Particulate Matter Derived from Coal Combustion, *Energy & Fuels* **2002**, *16*, 325–329.
6. Galbreath, K.C.; Toman, D.L.; Zygarlicke, C.J.; Pavlish, J.H. Trace Element Partitioning and Transformations During Combustion of Bituminous and Subbituminous U.S. Coals in a 7-kW Combustion System. *Energy & Fuels* **2000**, *14*, 1265–1279.
7. Galbreath, K.C.; Zygarlicke, C.J.; Huggins, F.E.; Huffman, G.P.; Wong, J. Chemical Speciation of Nickel in Residual Oil Ash. *Energy & Fuels* **1998**, *12 (4)*, 818–822.
8. Galbreath, K.C.; Toman, D.L.; Zygarlicke, C.J.; Huggins, F.E.; Huffman, G.P.; Wong, J. Nickel Speciation of Residual Oil Fly Ash and Ambient Particulate Matter Using X-Ray Absorption Spectroscopy. *J. Air & Waste Manage. Assoc.* **2000**, *50 (11)*, 1876–1886.
9. Huffman, G.P.; Huggins, F.E.; Shah, N.; Huggins, R.; Linak, W.P.; Miller, C.A.; Pugmire, R.J.; Meuzelaar, H.L.C.; Seehra, M.S.; Manivannan, A. Characterization of Fine Particulate Matter Produced by Combustion of Residual Fuel Oil. *J. Air & Waste Manage. Assoc.* **2000**, *50*, 1106–1114.
10. Nickel Producers Environmental Research Association (NiPERA). Occupational Exposure Limits Criteria Document for Nickel and Nickel Compounds, Volume 1: Summary, Conclusions, and Recommendations. Prepared for the European Commission, Directorate-General V, Public Health and Safety at Work Directorate. Prepared by NiPERA in collaboration with Eurometaux, Dec 24, 1996.
11. Toxicology Excellence for Risk Assessment (TERA). Toxicological Review of Soluble Nickel Salts. Prepared for the Metal Finishing Association of Southern California, Inc., U.S. Environmental Protection Agency, and Health Canada. Prepared by TERA under subcontract in part with Science Applications International Corporation, EPA Contract No. 68-C7-0011, March 1999.

12. *Provisions for Attainment and Maintenance of National Ambient Air Quality Standards*; U.S. Public Law, 101-549, 1990.
13. U.S. Environmental Protection Agency. *National Ambient Air Quality Standards (NAAQS)*, <http://www.epa.gov/airs/criteria.html> (accessed May 8, 2003), Washington, DC, Nov 2002.
14. U.S. Environmental Protection Agency. *National Air Toxics Program: The Integrated Urban Strategy*. <http://www.epa.gov/ttn/atw/urban/urbanpg.html> (accessed May 7, 2003), Washington, DC, July 1999.
15. U.S. Environmental Protection Agency. *1996 Toxics Release Inventory, Public Data Release—Ten Years of Right-to-Know*; EPA 745-R-08-005, Washington, DC, May 1998.
16. Kashireninov, O.E.; Fontijn, A. Modeling of Chromium Combustion in Incineration: Thermochemistry of Cr-C-H-Cl Combustion in Air and Selection of Key Reactions. *Comb. and Flame* **1998**, *113*, 498–506.